Published in final edited form as:
Science. 2009 June 26; 324(5935): 1726–1729. doi:10.1126/science.1171716.

Solution NMR Structure of Membrane-Integral Diacylglycerol Kinase

Wade D. Van Horn[1,*], **Hak-Jun Kim**[1,2,*], **Charles D. Ellis**[1], **Arina Hadziselimovic**[1], **Endah S. Sulistijo**[1], **Murthy D. Karra**[1], **Changlin Tian**[1,3], **Frank D. Sönnichsen**[4], and **Charles R. Sanders**[1,†]

[1] Dept. of Biochemistry and Center for Structural Biology, Vanderbilt University, Nashville, TN 37232, USA

[2] Korea Polar Research Institute, Incheon, 406-840, Korea

[3] School of Life Science, University of Science and Technology of China, Hefei, Anhui, 230026, P. R. China

[4] Otto Diels Institute for Organic Chemistry, Christian Albrechts University of Kiel, Germany

Abstract

Escherichia coli diacylglycerol kinase (DAGK) represents a family of integral membrane enzymes that is unrelated to all other phosphotransferases. We have determined the three-dimensional structure of the DAGK homotrimer using solution NMR. The third transmembrane helix from each subunit is domain-swapped with the first and second transmembrane segments from an adjacent subunit. Each of DAGK's three active sites resembles a portico. The cornice of the portico appears to be the determinant of DAGK's lipid substrate specificity and overhangs the site of phosphoryl transfer near the water-membrane interface. Mutations to cysteine that caused severe misfolding were located in or near the active site, indicating a high degree of overlap between sites responsible for folding and for catalysis.

E. coli DAGK is encoded by the *dgkA* gene and catalyzes direct phosphorylation of diacylglycerol (DAG) by MgATP to form phosphatidic acid as part of the membrane-derived oligosaccharide (MDO) cycle(1–3). In Gram-positive organisms, the *dgkA* homolog encodes an undecaprenol kinase, indicating a role in oligosaccharide assembly or in related signaling pathways(4). The DAGK homolog in *Streptoccus mutans* is known to be a virulence factor for smooth surface dental caries(5). DAGK was among the first integral membrane enzymes to be solubilized, purified, and mechanistically characterized(6). The wild type protein is very stable (7,8) and can spontaneously insert into lipid bilayers to adopt its functional fold(9,10). Paradoxically, DAGK resembles many disease-linked human membrane proteins because it is highly susceptible to mutation-induced misfolding(10–12). DAGK functions as a 40 kDa homotrimer, with a total of nine transmembrane (TM) helices and three active sites(13).

†To whom correspondence should be addressed. chuck.sanders@vanderbilt.edu.
*These authors contributed equally to this work.

Supporting Online Material
www.sciencemag.org/cgi/content/full…
Materials and Methods
Figs. S1-S8
Tables S1-S4

The structure of DAGK was determined using solution NMR methods(14) under conditions in which the enzyme is a functional homotrimer solubilized in ca. 100 kDa dodecylphosphocholine micelles, work that extends other solution NMR studies of >20kDa multi-span membrane proteins (15–22). The backbone structure of the helical TM domain of DAGK (residues 26–121) was precisely determined by the data (Fig. 1, fig. S1 and table S4); however, motions associated with the N-terminus (residues 1–25) have hindered determination of its conformation beyond confirming the presence of two stable amphipathic helices.

DAGK's structure bears no resemblance to that of the water soluble DAGK(23) (Fig. 1). The three-fold symmetry axis lies at the center of a parallel left-handed bundle formed by the second transmembrane (TM2) helices of the three subunits. TM2 has previously been proposed to play a central role in DAGK's folding and stability(24,25) and contains several highly conserved residues (Fig. 1), particularly near the membrane/cytoplasm interface. Characterization of a series of cysteine-replacement mutants for sites in TM2 showed that mutations in this segment often resulted in a dramatic reduction in catalytic function (Fig. 2 and table S1), underscoring the importance of TM2 to DAGK folding and catalysis.

DAGK is seen to be a domain-swapped homotrimer (Fig. 1C). TM3 makes virtually no contact with TM2 from the same subunit. Instead, it packs against the hairpin formed by the first and second TM segments from an adjacent subunit (TM1′ and TM2′). Domain-swapping may contribute to the high stability of wild type DAGK(7,8). Conversely, domain-swapping may illuminate why DAGK mutants are often difficult to refold following denaturation(11).

A distinctive structural feature of the DAGK structure is a membrane-submerged cavity that resembles a portico (Figs. 1A and 2B and fig. S1). TM1 and TM3 serve as the pillars that bound the entry, terminating at an inner wall formed by TM2′ from a neighboring subunit, and crowned by an overhanging cornice comprised of the connecting loop between TM2 and TM3. The portico, and in particular the cornice, contains a majority of the residues seen to be functionally essential in our mutagenesis studies (Fig. 2). Each portico contains functionally-critical residues that are contributed by two different subunits, consistent with a previous mutagenesis study which showed that each active site is shared between subunits (13). Titrations of DAGK with its substrates/products (MgATP, DAG, and phosphatidic acid) and with a non-hydrolyzable ATP analog (β, γ-methyleneadenosine 5′-triphosphate, AMP-PCP) were monitored by NMR. Significant and saturable changes in NMR resonances upon ligand binding (Fig. 3 and fig. S5) confirmed that the portico includes the lipid substrate binding site of DAGK. The overhanging cornice likely blocks lateral diffusion into the active site of lipids with head groups larger than DAG and phosphatidic acid. On the other hand, the spaciousness of the lower part of the portico explains the lack of specificity of DAGK with respect to the acyl chain composition of diglyceride substrates (26). Interactions of membrane enzymes with membranous substrates more typically involve gated internal cavities within the protein or well-structured grooves that confer high specificity for specific substrates (27–29), although the active site of the homodimeric beta-barrel outer membrane phospholipase A also exhibits a portico-like architecture, consistent with the lack of specificity of this enzyme in terms of substrate acyl chains(27,30).

NMR resonances for three residues located just under the cornice on TM1 and TM2′ exhibit significant shifts in response to the binding of nucleotides and lipids (Fig. 3). These sites are likely proximal to the site of ATP-to-DAG phosphoryl transfer, consistent with the observed proximity to the cornice of many of the highly conserved and functionally-critical residues. We suggest that a second role for the cornice in the active site may be to seal off the substrate-filled active site from water (to avoid ATP hydrolysis), a catalytic imperative that is usually satisfied in water soluble phosphotransferases, such as adenylate kinase, by global domain motions that close the active site upon substrate binding(31). DAGK appears not to undergo a

global conformational change, as revealed by observation of only modest and highly localized changes in NMR resonance positions for DAGK upon forming binary complexes with its substrates or with a ternary complex with DAG and MgAMP-PCP (Fig. 3 and fig. S5).

As alluded to above, we systematically examined the functional consequences of mutating each residue in DAGK to cysteine to gain insight into structure-function relationships beyond what can be deduced either from multiple sequence alignment or from a previous phenotype-based random mutagenesis study(32). Mutants that resulted in >85% loss of catalytic activity (listed in table S1) were further characterized to reveal two categories of defects (details in table S2 and summary in Fig. 2). First are mutations that do not disrupt protein folding, but result in loss of catalytic function. These residues are either directly in the active site or play specific local structural roles in support of the active site. Second are mutations to cysteine that result in misfolding so severe that *in vivo* expression levels were seen to be reduced (Fig. 2 and table S2), often to an undetectable level. In cases where purification was possible, such mutants were typically observed to be aggregation-prone (table S2). While cysteine-scanning mutagenesis is a commonly used in studies of membrane proteins (c.f. 33), we are unaware of previous documentation of a set of mutants analogous to the misfolding-prone variants described in this work.

A remarkable feature of the DAGK structure is the close proximity between the active site and a majority of residues for which mutations to cysteine result in severe misfolding (Fig. 2 and table S2). This is in contrast with enzymes, such as those of the TIM barrel superfamily(34), where the active site is set within a robust structural framework that is tolerant of major remodeling of catalytic residues. Given that numerous diseases, such as cystic fibrosis, are associated with inherited or sporadic mutations that result in single amino acid changes in membrane protein sequence(12), our results serve as a warning that even for a structurally well-characterized membrane protein, knowledge regarding the location of a disease-promoting mutation site cannot *a priori* be used to reliably predict the exact nature of the molecular defect that is linked to disease etiology (i.e., local active site disruption vs. catastrophic misfolding).

That most of the residues important for avoiding misfolding of DAGK are located at the DAGK active site suggests that the portico is unlikely to be adapted by evolution to orthologous functions. While DAGK has been shown to be a highly efficient catalyst in its microbial physiological niche(3), intimate linkage between activity and folding may help to explain why this enzyme is an evolutionary orphan.

Supplementary Material

Refer to Web version on PubMed Central for supplementary material.

References and Notes

1. Kennedy EP. Proc Natl Acad Sci U S A 1982;79:1092. [PubMed: 7041113]
2. Raetz CR, Newman KF. J Bacteriol 1979;137:860. [PubMed: 217867]
3. Badola P, Sanders CR. J Biol Chem 1997;272:24176. [PubMed: 9305868]
4. Lis M, Kuramitsu HK. Infect Immun 2003;71:1938. [PubMed: 12654811]
5. Shibata Y, et al. Microbiology 2009;155:557. [PubMed: 19202104]
6. Walsh JP, Bell RM. Methods Enzymol 1992;209:153. [PubMed: 1323028]
7. Lau FW, Bowie JU. Biochemistry 1997;36:5884. [PubMed: 9153430]
8. Zhou Y, Bowie JU. J Biol Chem 2000;275:6975. [PubMed: 10702260]
9. Lorch M, Booth PJ. J Mol Biol 2004;344:1109. [PubMed: 15544815]
10. Nagy JK, Sanders CR. Biochemistry 2004;43:19. [PubMed: 14705927]
11. Gorzelle BM, et al. Biochemistry 1999;38:16373. [PubMed: 10587463]

12. Sanders CR, Myers JK. Annu Rev Biophys Biomol Struct 2004;33:25. [PubMed: 15139803]
13. Lau FW, Chen X, Bowie JU. Biochemistry 1999;38:5521. [PubMed: 10220339]
14. Full description of materials and methods are available as supporting material on *Science* Online. Briefly, the backbone structure of micellar DAGK at pH 6.5 was determined using ^{1}H-^{1}H nuclear Overhauser effect-derived distances, backbone torsion angle restraints from chemical shifts, residual dipolar couplings, and paramagnetic relaxation effect-derived distances. These NMR restraints were also supplemented by a limited number of intersubunit inter-residue distance restraints derived from disulfide mapping measurements that employed single-cysteine mutant forms of DAGK. Care was taken to avoid possible motional complications to the disulfide mapping-derived distances. The structure was calculated using standard restrained molecular dynamics and simulated annealing protocols.
15. Oxenoid K, Chou JJ. Proc Natl Acad Sci U S A 2005;102:10870. [PubMed: 16043693]
16. Zhou Y, et al. Mol Cell 2008;31:896. [PubMed: 18922471]
17. Bayrhuber M, et al. Proc Natl Acad Sci U S A 2008;105:15370. [PubMed: 18832158]
18. Hiller S, et al. Science 2008;321:1206. [PubMed: 18755977]
19. Liang B, Tamm LK. Proc Natl Acad Sci U S A 2007;104:16140. [PubMed: 17911261]
20. Ma D, et al. Proc Natl Acad Sci U S A 2008;105:16537. [PubMed: 18948596]
21. Baker KA, Tzitzilonis C, Kwiatkowski W, Choe S, Riek R. Nat Struct Mol Biol 2007;14:1089. [PubMed: 17922011]
22. Chill JH, Louis JM, Miller C, Bax A. Protein Sci 2006;15:684. [PubMed: 16522799]
23. Miller DJ, Jerga A, Rock CO, White SW. Structure 2008;16:1036. [PubMed: 18611377]
24. Nagy JK, Lau FW, Bowie JU, Sanders CR. Biochemistry 2000;39:4154. [PubMed: 10747807]
25. Partridge AW, Melnyk RA, Yang D, Bowie JU, Deber CM. J Biol Chem 2003;278:22056. [PubMed: 12686537]
26. Walsh JP, Fahrner L, Bell RM. J Biol Chem 1990;265:4374. [PubMed: 2155227]
27. Bishop RE. Biochim Biophys Acta 2008;1778:1881. [PubMed: 17880914]
28. Lemberg MK, Freeman M. Mol Cell 2007;28:930. [PubMed: 18158892]
29. Martinez MD, et al. Nature 2007;448:613. [PubMed: 17632546]
30. Snijder HJ, et al. Nature 1999;401:717. [PubMed: 10537112]
31. Kumar S, Ma B, Tsai CJ, Wolfson H, Nussinov R. Cell Biochem Biophys 1999;31:141. [PubMed: 10593256]
32. Wen J, Chen X, Bowie JU. Nat Struct Biol 1996;3:141. [PubMed: 8564540]
33. Kaback HR, Sahin-Toth M, Weinglass AB. Nat Rev Mol Cell Biol 2001;2:610. [PubMed: 11483994]
34. Nagano N, Orengo CA, Thornton JM. J Mol Biol 2002;321:741. [PubMed: 12206759]
35. Oxenoid K, Kim HJ, Jacob J, Sonnichsen FD, Sanders CR. J Am Chem Soc 2004;126:5048. [PubMed: 15099070]
36. We thank James Bowie for providing the DAGK expression system, many of the mutants employed in this work, and much discussion. We thank Markus Voehler, Bonnie Gorzelle, Peter Power, Congbao Kang, and Jason Jacob for technical assistance and Kirill Oxenoid, Lewis Kay, Scott Prosser, Ming-Daw Tsai, Tina Iverson, Jens Meiler, Anthony Forster, John Battiste, Walter Chazin and members of the Sanders lab for discussion. This work was supported by NIGMS/NIH RO1 GM47485, with WVH receiving training support by NIH T32 NS007491. The coordinates for DAGK have been deposited as PDB entry 2kdc in the Protein Data Bank. This work is dedicated to the fond memory of Anne Karpay.

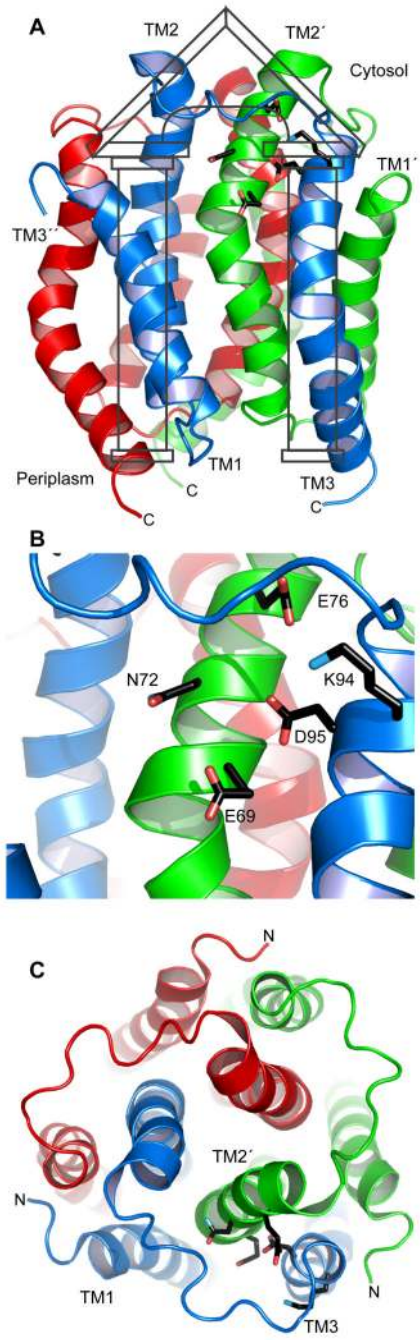

Figure 1.

Structure of diacylglycerol kinase. All panels are for the same representative conformer from the ensemble of structures (fig. S1). Omitted from this figure is the N-terminus (residues 1–25), which was not precisely determined, although it is known to be comprised of two short α-helices that extend over residues 6–14 and 17–23. **(A)** Ribbon diagram of DAGK with inscribed portico viewed from the membrane plane. DAGK's five most highly conserved residues are shown (for a single portico only) **(B)** Ribbon diagram viewed from the membrane plane showing a close-up of the region of the active site containing DAGK's most highly conserved residues. **(C)** Ribbon diagram viewed from the cytosol showing side chains for DAGK's 5 most highly conserved residues (for a single portico only). The connecting loops

between the first and second TM segments have been omitted from view so that the organization of the TM helices can more easily be discerned.

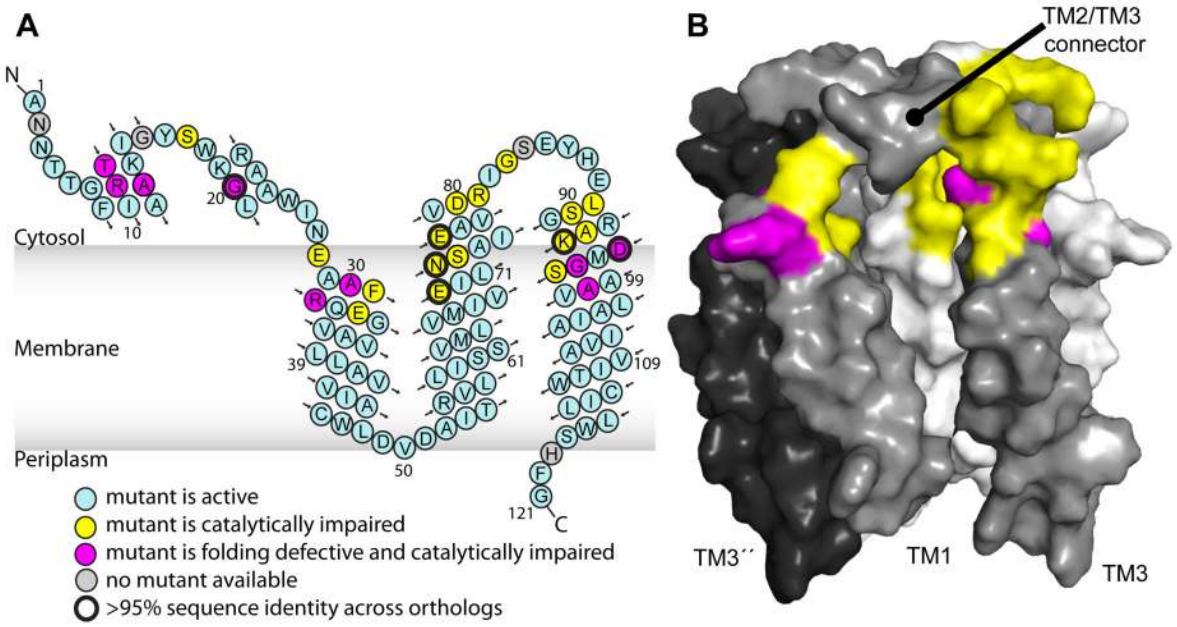

Figure 2.

Identification of sites critical for catalysis and/or for folding based on the functional analysis of mutants generated by systematically replacing each residue in DAGK with cysteine. **(A)** Sites labeled blue designate cysteine mutants that exhibited at least 20% of wild type activity. Yellow labels indicate sites for which mutants were observed to fold, but that exhibited less than 20% catalytic activity. Mutation to cysteine at the pink sites resulted in forms of DAGK that were both inactive and misfolded, both in native *E. coli* membranes and following purification and application of normally-effective refolding protocols. Residues highlighted in the surface-filled representation of DAGK **(B)** are for a single portico site only (residues are highlighted only for TM1, TM3 and TM2′). Omitted from the surface representations are the imprecisely determined N-termini (residues 1–25). Specific activities for each mutant are listed in table S1. Details of the folding behavior of mutants that exhibit <15% of wild type activity are given in table S2. Sites that are indicated as being conserved with >95% identity were identified based on the multiple sequence alignment presented in figs. S2–S3.

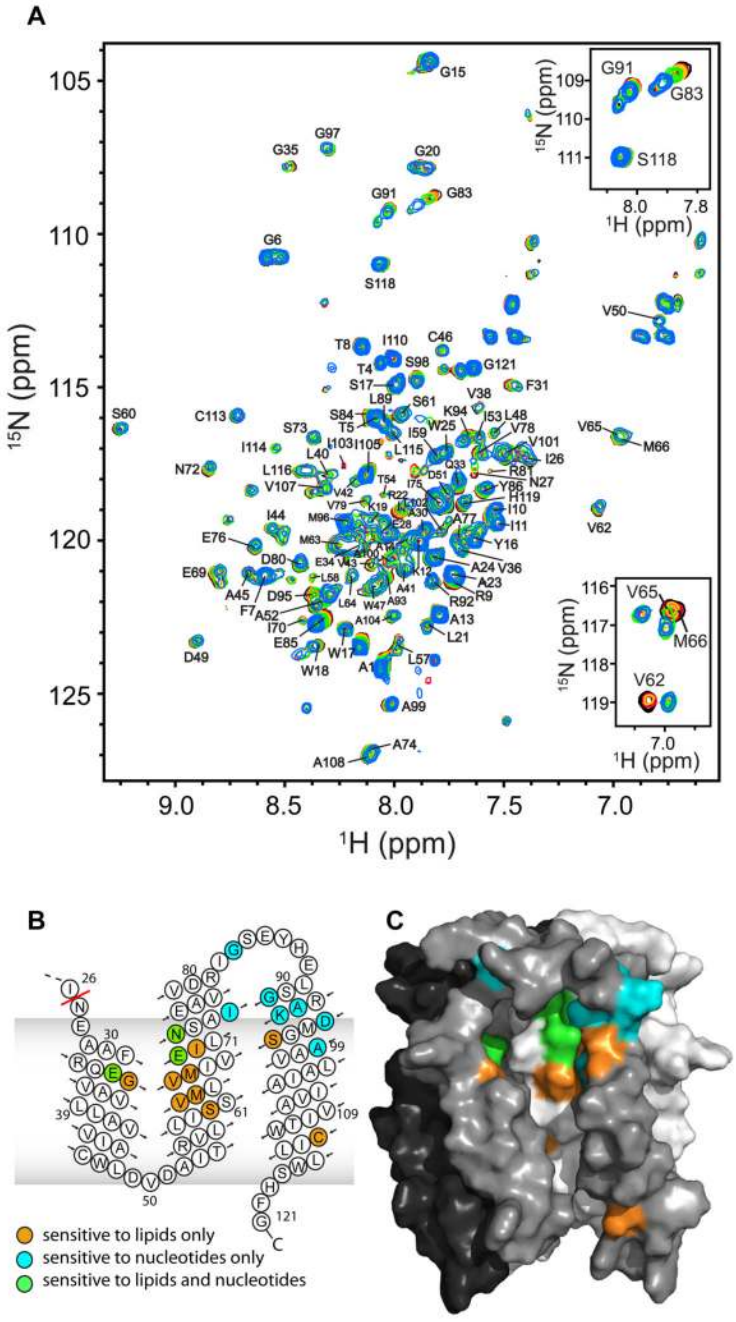

Figure 3.

NMR mapping of the substrate binding sites. **(A)** Example of 800 MHz ^{1}H, ^{15}N-TROSY NMR spectra used to monitor titration of wild type DAGK by a substrate/product or substrate analog. Shown are the overlaid spectra for titration of DAGK by MgAMP-PCP at concentrations of 0 mM (black), 2 mM (red), 4 mM (yellow), 8 mM (green), and 16 mM (blue). Resonances are labeled based on their residue assignments (35). Unlabeled peaks reflect the 10% of resonances for which assignments were not completed. NMR data for titrations of DAGK with DAG, phosphatidic acid, and MgATP are shown in fig. S5. **(Insets to A)** Selected peaks from the MgAMP-PCP titration (upper panel) and from a separate DAG titration (lower panel, see full spectra in fig. S5). The MgAMP-PCP data illustrate fast exchange NMR conditions in which

DAGK peaks gradually change position during the titration, reflecting population-weighted averages between free and complexed forms. In contrast, the data from the DAG titration (lower panel) illustrates slow exchange behavior, where the free enzyme peaks disappear and peaks representing the complex appear at new positions, with contour intensities reflecting the relative populations of the free and complexed states. **(B)** Summary of active site mapping, highlighting residues associated with TROSY resonances that exhibit large and saturable changes in positions in response to substrate/analog binding. **(C)** Structure of DAGK with residues highlighted for which TROSY resonances exhibited significant and saturable changes in chemical shift upon binding. In blue are residues that are perturbed by addition of MgATP or MgAMP-PCP ($\Delta\delta > 0.02$ PPM) and in orange are those perturbed by addition of DAG ($\Delta\delta > 0.025$ PPM). Residues for which resonance positions are perturbed by both nucleotide and lipid titrations are green.